



Microscopic molecular mobility of amorphous AG-041R measured by solid-state ^{13}C NMR

Akiko Koga^{a,b}, Etsuo Yonemochi^a, Minoru Machida^b, Yoshinori Aso^b,
Hidetoshi Ushio^c, Katsuhide Terada^{a,*}

^a Department of Pharmaceutics, School of Pharmaceutical Sciences, Toho University, 2-2-1 Miyama, Funabashi, Chiba 274-8510, Japan

^b Pre-Clinical Research Department 1, Chugai Pharmaceutical Co. Ltd., 1-135 Komakado, Gotemba, Shizuoka 412-8513, Japan

^c Quality Assurance Department, Chugai Pharmaceutical Co. Ltd., 5-5-1 Ukima, Kita-ku, Tokyo 115-8543, Japan

Received 6 September 2003; received in revised form 15 January 2004; accepted 20 January 2004

Abstract

Purpose: AG-041R is characterized to be stable in amorphous state and difficult to crystallize at normal period of time. In order to investigate the molecular mobility in microscopically, the spin–lattice relaxation time (T_1) of AG-041R was investigated by solid-state CP/MAS ^{13}C NMR at temperature below and above glass transition temperature (T_g). **Method:** CP/MAS measurement and T_1 measurement were performed by means of ^{13}C NMR, where the measurement temperatures were 60, 70, 80, 100, and 110 °C. The spin–lattice relaxation time (T_1) of AG-041R was calculated from the relaxation curves. **Results:** From the analysis of T_1 of amorphous AG-041R, it was clarified that all of the carbons did not start moving drastically at T_g and there were some groups of carbon in terms of temperature dependency of T_1 . One is a type, such as the carbons in benzene ring: their T_1 was drastically changed at T_g . On the other hand, T_1 of carbonyl carbons gradually decreased, and above T_g their T_1 was still higher than that of the other carbons. There was no significant change of T_1 in the methyl carbons around T_g . From the study of IR and ^1H NMR in solution, the inter- and intramolecular hydrogen bondings between NH and C=O were found in AG-041R. Due to hydrogen bonding, the inter- and/or intramolecular interaction is considered to retain even at supercooled liquid state. **Conclusion:** The structure that contributes glass transition is the main skeleton structure, such as benzene ring, while small group, like methyl, start to move at lower temperature than T_g . On the other hand, for the carbons, such as carbonyl, their structure was restricted by inter- and/or intramolecular interaction, therefore, their molecular mobility was significantly low above T_g .

© 2004 Elsevier B.V. All rights reserved.

Keywords: Amorphous; Solid-state ^{13}C NMR; Relaxation; Molecular mobility

1. Introduction

Amorphous pharmaceuticals having largely higher free energy than any other crystalline forms have many advantages for the formulation of solid dosage forms,

such as improvement of solubility, enhancement of dissolution rate, and promotion of therapeutic activity (Yamaguchi et al., 1992; Jaeghere et al., 2000). However, the drawbacks of these pharmaceuticals are their chemical instability, which could lead to unfavorable effect on shelf-life. In order to manufacture the favorable amorphous pharmaceuticals, it is necessary to predict the chemical and physical stability of amorphous pharmaceuticals on the storage period of

* Corresponding author. Tel.: +81-47-472-1337;

fax: +81-47-472-1337.

E-mail address: terada@phar.toho-u.ac.jp (K. Terada).

time (Yoshioka et al., 1994; Matsumoto and Zografi, 1999). It is fundamental to achieve better understandings of the dynamics of molecular motion occurring amorphous pharmaceuticals (Hancock et al., 1999a,b; Schmitt et al., 1999), because molecular relaxation takes place during storage of the amorphous pharmaceuticals. The molecular mobility of amorphous pharmaceuticals and their stability have been reported for various analytical methods, such as differential scanning calorimetry (DSC) (Moynihan et al., 1974), thermal mechanical analysis (TMA) (Hancock et al., 1999a,b), and dielectric relaxation (Yoshioka et al., 1999). The thermal methods have been performed at temperature below and above T_g and macroscopic cooperative type of molecular motion was monitored as relaxation enthalpy. These macroscopic analyses, however, only observe an average mobility of whole molecule.

The spectroscopic researches about the relaxation behavior of amorphous pharmaceuticals have also been done by NMR (Aso et al., 2000; Wang et al., 1996; Shamblin et al., 2000). The spin–lattice relaxation time (T_1) and spin–spin relaxation time (T_2) have been measured for amorphous pharmaceuticals. However, few researches have been performed about microscopic performance of amorphous pharmaceuticals, such as molecular motion of functional groups.

In an attempt to gain better understanding of relaxation process in amorphous pharmaceuticals, it is assumed that the mobility of each functional group may act as different relaxation and may affect the physical stability of amorphous systems. This paper describes the macroscopic and microscopic molecular mobility of AG-041R measured by enthalpy relaxation time with DSC and relaxation of functional group by solid-state ^{13}C NMR.

2. Materials and methods

2.1. Materials

A newly synthesized cholecystokinin-B/gastrin receptor antagonist AG-041R, 3*R*-1-(2,2-diethoxyethyl)-3-((4methylphenyl)aminocarbonylmethyl)-3-((4methylphenyl)ureido-indoline-2-one) (Ding et al., 1997; Fukui et al., 1998), was used experimentally. The chemical structure of AG-041R is shown in Fig. 1.

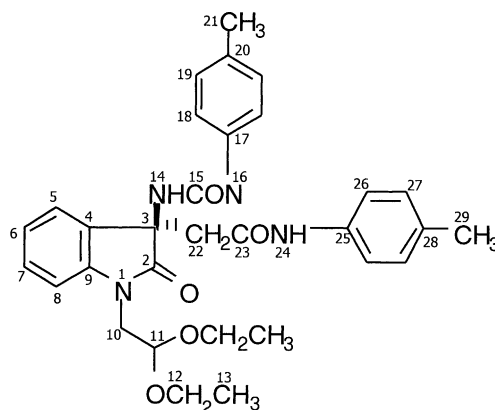


Fig. 1. Molecular structure of AG-041R.

Amorphous of AG-041R was prepared as a pale yellow powder by ether/hexane re-precipitation method. The glassy-state AG-041R, which has no thermal history, was prepared by cooling at 20 °C/min from 160 to 30 °C in DSC cell. Chloroform was purchased from WAKO Chemical Company (Japan). *d*-Chloroform was purchased from MERCK Chemical Company.

2.2. Methods

The thermal characteristics were investigated by means of DSC (DSC7, Perkin Elmer) with heating rate of 20 °C/min. Samples of AG-041R were weighted into aluminum pan (Perkin Elmer). To study enthalpy relaxation, AG-041R was heated in a cell of DSC or in the air thermostat at 60 °C. Nitrogen gas was used as the purge gas.

The molecular conformation including existence of intra/intermolecular hydrogen bond was studied in chloroform or *d*-chloroform using FT-IR (FT-730, HORIBA) and ^1H NMR (EX-270, JEOL). Sample concentrations were in the range of 2.5–40 mM for FT-IR and 0.8–30 mM for ^1H NMR. The internal reference in ^1H NMR was TMS. The solid-state FT-IR was measured with KBr by Diffuse Reflectance Analysis (DRA) method using DRA unit (Spectra Tech). The range of FT-IR spectra was from 400 to 4000 cm^{-1} .

CP/MAS measurement and T_1 measurement were performed by means of ^{13}C NMR (CMX-300 Infinity, Chemagnetics), where the measurement temperatures were 60, 70, 80, 100, and 110 °C and waiting times

were 110 μ s, 100, 500 ms, 1, 3, 5, 10, 20, 35, and 50 s. Data were analyzed using the Spinsight software.

3. Results and discussion

3.1. Confirmation of the physical stability of AG-041R by macroscopic relaxation using thermal analysis

AG-041R was characterized by the powder X-ray diffraction and DSC methods. The distinct diffraction peaks due to crystals were not observed by the powder X-ray diffraction. The DSC curves did not show endothermic behavior due to melting, however, exhibited a small jump of heat capacity due to glass transition at about 90 °C. The solid-state AG-041R was identified to be amorphous. Amorphous is a non-equilibrium state that will be occurred due to relaxation during storage. In order to study the molecular mobility of amorphous AG-041R in macroscopic view, the enthalpy relaxation phenomenon was investigated by DSC. The enthalpy relaxation of AG-041R was measured at 60 °C using freshly prepared sample. Fig. 2 shows the enthalpy recovery of amorphous AG-041R stored at 60 °C for 10 months. The peak area depicted in DSC curve represents the enthalpy recovery related to the amount of relaxation of amorphous AG-041R. The enthalpy recovery associated with the relaxation amount increased with storage time. In order to study the molecular mobility of AG-041R, the molecular re-

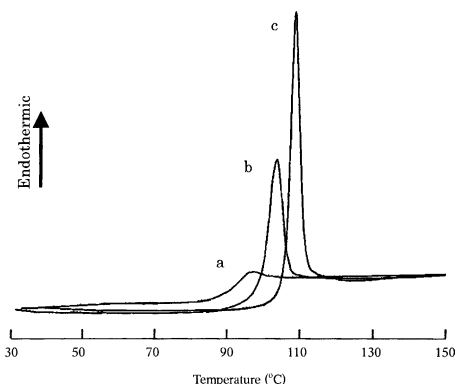


Fig. 2. Enthalpy recovery of amorphous AG-041R stored at 60 °C for 10 months; (a) after cooling, (b) stored for 3 days, (c) stored for 10 months.

laxation time constant (τ) was evaluated using the data of the enthalpy recovery. The molecular relaxation process is typically non-exponential and is usually analyzed by Kohlrausch–Williams–Watts (Williams and Watts, 1970; Shamblin et al., 2000) equation.

The extent of relaxation was calculated from the following equation:

$$\phi(t) = 1 - \frac{\Delta H(t)}{\Delta H(\infty)} \quad (1)$$

where $\Delta H(t)$ and $\Delta H(\infty)$ are measured enthalpy recovery at time t and maximum enthalpy recovery, respectively. For $\phi(t)$, empirical equation of Kohlrausch–Williams–Watts was applicable to enthalpy relaxation.

$$\phi(t) = \exp(-t/\tau)^\beta \quad (2)$$

where t is the storage time, τ is the relaxation time constant, and β is a relaxation time distribution parameter.

The relaxation function of glassy AG-041R at 60 °C was calculated from Eqs. (1) and (2) using non-linear regression. Consequently, $\Delta H(\infty)$ was calculated to be 17.9 J/g. The relaxation time (τ) was estimated to be 1440 h with exponential function (τ) of 0.29. The relaxation time of amorphous AG-041R is extremely longer than that of other pharmaceuticals, such as indomethacin, having the relaxation time of 2.4 h at 30 °C. Therefore, we have confirmed that AG-041R would be significantly stable in amorphous state under conventional storage period. The thermal analysis measures overall relaxation process and measures the average relaxation time. To clarify the good stability of AG-041R, the microscopic relaxation measurement was performed in the following section.

3.2. Microscopic relaxation of AG-041R

3.2.1. Molecular conformation of AG-041R

In the research of relaxation of amorphous solid, evaluation of the molecular conformation of AG-041R in amorphous state gives important information concerning the microscopic movement of molecule. The solution spectra of IR and NMR were measured to speculate the molecular conformation of AG-041R in amorphous state. Fig. 3 shows the IR spectra of $\nu(\text{N-H})$ region of AG-041R with different concentrations of AG-041R in chloroform solution. The peak

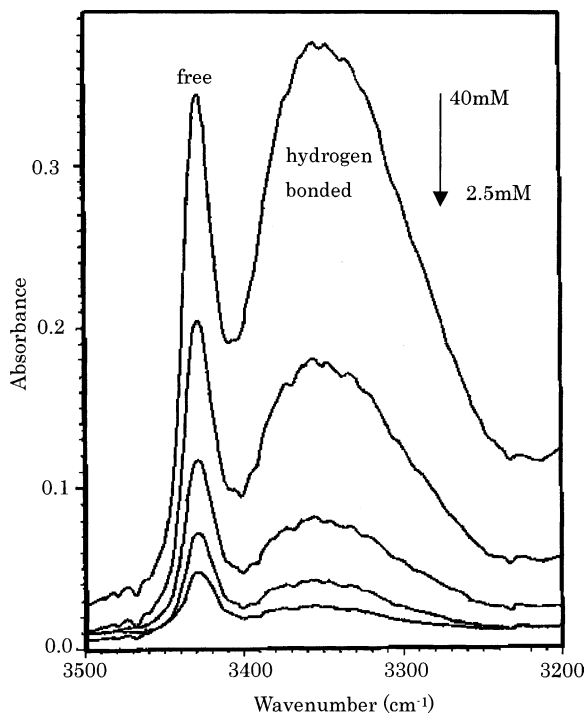


Fig. 3. The IR spectra of 40, 20, 10, 5, and 2.5 mM AG-041R chloroform solution in the region from 3500 to 3200 cm^{-1} .

at 3429 cm^{-1} was assigned to free $\nu(\text{N-H})$ and the peak at 3356 cm^{-1} was assigned to hydrogen bonded $\nu(\text{N-H})$. The hydrogen bonded $\nu(\text{N-H})$ was still remained as low concentration as 2.5 mM. Furthermore, three amide I absorbance bands (around 1700 cm^{-1} , C2=O, C15=O, C23=O) were changed with concentration as well (data not shown). The C=O peaks observed around 1700 cm^{-1} were overlapped; therefore, it was very difficult to assign the peaks of the samples. From the change in the intensity of hydrogen bonded N-H and C=O in IR spectra, the formation of the intra- and intermolecular hydrogen bondings were assumed in the AG-041R molecules.

The ^1H NMR spectra of AG-041R were also measured with the different concentrations of AG-041R in *d*-chloroform solution. Fig. 4 shows the chemical shifts of three N-H groups at different concentrations. Although the chemical shifts of amide at N14 was not observed, the downfield chemical shifts of amides at N24 and N16 were observed with increasing concentration. From the IR and ^1H NMR spectra, we have confirmed that intermolecular hydrogen bonding was

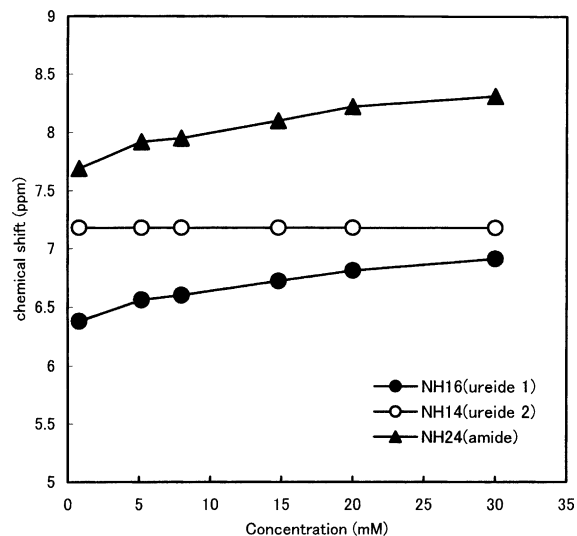


Fig. 4. The ^1H NMR chemical shifts of N-H of AG-041R in CDCl_3 .

formed at N16 with C2=O or C15=O and N24 with C2 or C15, and intramolecular hydrogen bonding was formed at N14 with C23=O. The chemical shift of N24 was greater than that of N16, suggesting that the molecular interaction between N24 and C2=O or C15=O would be stronger than that between N16 and the carbonyl groups.

3.2.2. Solid-state ^{13}C NMR spectra of AG-041R

NMR spectra in the solid state provide some information regarding the local environment of individual carbons. In order to investigate the molecular mobility of amorphous AG-041R microscopically, CP/MAS ^{13}C NMR was measured at temperature below and above T_g . Fig. 5 shows the CP/MAS ^{13}C NMR spectra of AG-041R measured at temperatures ranging from 60 to 110°C . The assignment of each signal was compared to C-H COSY solution spectra and the chemical shift of each carbon was depicted in the CP/MAS ^{13}C NMR spectra. In the CP/MAS ^{13}C NMR spectra, the distinct change in chemical shifts was not observed both below (60, 70, and 80°C) and above (100 and 110°C) T_g . However, the increase in sharpness of each signal was observed above T_g . It is considered that the prominent structural change, such as crystallization of amorphous, did not take place at these temperatures.

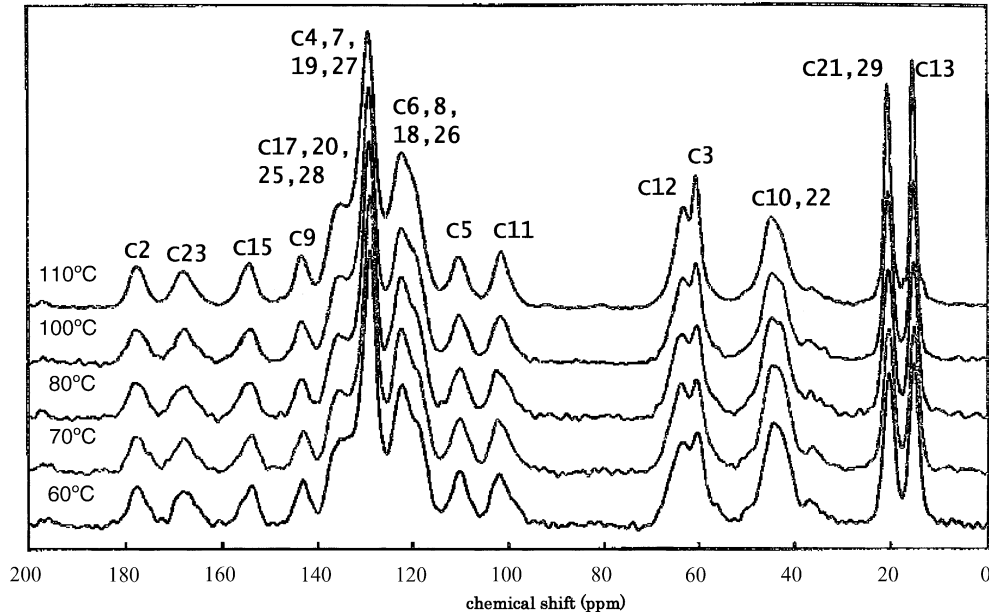


Fig. 5. The CP/MAS ^{13}C NMR spectra of AG-041R measured at temperatures ranging from 60 to 110°C.

3.2.3. Temperature dependency of relaxation time (T_1) of AG-041R

The molecular mobility of each functional group was determined from CP/MAS ^{13}C NMR relaxation time at below (60, 70, and 80°C) and above (100 and 110°C) T_g . The microscopic mobility of each functional group was evaluated on the basis of relaxation time. The spin–lattice relaxation time (T_1) of AG-041R was calculated from relaxation curves. Fig. 6 shows the relaxation curves of quaternary carbon (C3) at 60 and 110°C. The relaxation at 110°C was faster than that at 60°C, suggesting the existence of the temperature dependency of the relaxation rate. The relaxation curve of signal intensity was fitted to

two exponential functions, which is related to slow relaxation process and fast relaxation process.

$$I(t) = I^S \exp(-t/T_1^S) + I^F \exp(-t/T_1^F) \quad (3)$$

where superscripts (S and F) show the slower and faster relaxation processes, and $I(t)$ is a signal intensity at time t , I^S , and I^F are the signal intensity, and T_1^S and T_1^F are the relaxation time due to the slower and faster relaxation processes, respectively. Table 1 shows the relaxation time and signal intensity of slow and fast relaxation processes of quaternary carbon (C3). The slow and fast relaxation times of C3 at 60°C were determined as 119 and 1.9 s, and the signal intensity of each process was obtained as 1767.3 and 698.6,

Table 1
Relaxation time and signal intensity of slow and fast relaxation processes of quaternary carbon (C3)

Temperature (°C)	Relaxation time (s)		Signal intensity			
	Slow (T_1^S)	Fast (T_1^F)	Slow (I^S)	Fast (I^F)	$I^S/(I^S + I^F)$	$I^F/(I^S + I^F)$
60	119.3	1.9	1767.3	698.6	0.72	0.28
70	71.9	1.2	1540.5	777.2	0.66	0.34
80	72.1	1.8	1606.6	501.9	0.76	0.24
100	30.7	2.7	1805.6	592.8	0.75	0.25
110	28.2	1.7	1990.1	594.6	0.77	0.23

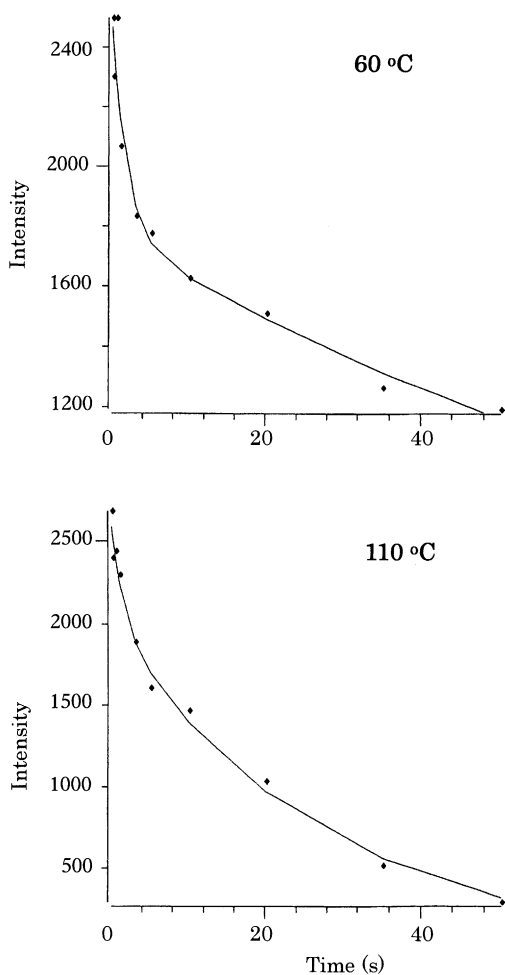


Fig. 6. Relaxation curves of C3 at 60 and 110 °C.

respectively. At the temperature of 110 °C, the slow relaxation time was decreased to 28.2 s. On the other hand, the fast relaxation time was not altered. In spite of the drastic change of the relaxation time by heating, there was no significant change in the ratios of peak intensity, $I^F/(I^S + I^F)$ and $I^S/(I^S + I^F)$.

Fig. 7 shows the change in relaxation time of each carbon of AG-041R as a function of temperature. The difference of relaxation time between at 60 °C and at each temperature ($-\Delta T_1: T_1(60^\circ\text{C}) - T_1(\text{any temperature})$) was plotted against temperature. The significant change in the relaxation time due to the benzene ring was observed at 90 °C suggesting the molecular mobility was changed at the T_g of AG-

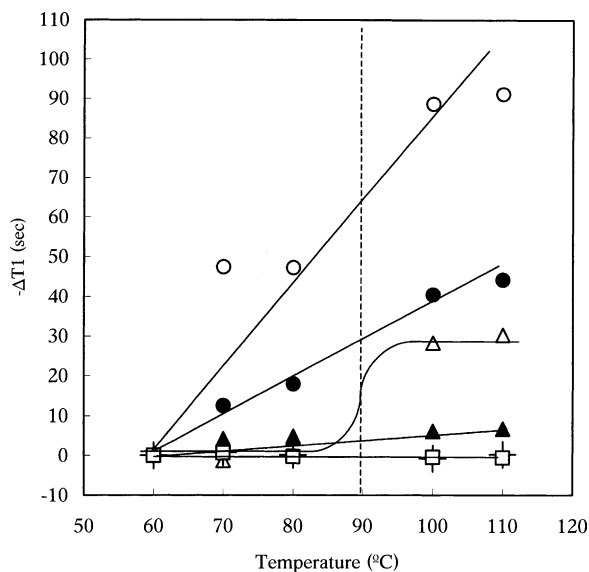


Fig. 7. Variation of relaxation time of each carbon of AG-041R as a function of temperature; (○) quaternary (C3) (T^S), (●) carbonyl (C2, 15, 23), (△) benzene ring (C4–9, 17–20, 25–28), (▲) methyl (C29, 21), (+) quaternary (C3), (□) methyl (C13).

041R. However, no significant change was observed in the other carbons, and there were some groups of carbon in terms of temperature dependency of T_1 . One is a type, such as the carbons in benzene ring (values plotted by symbol '△' in Fig. 7 are the mean data of benzene ring carbons): their T_1 was drastically changed at T_g . On the other hand, T_1 of carbonyl carbons gradually decreased, and above T_g their T_1 was still higher than that of the other carbons. There was no significant change of T_1 in the methyl carbons around T_g . The quaternary carbons showed two T_1 : the slower component (T_1^S) was similar to the carbonyl carbons, on the other hand, the faster component (T_1^F) was independent of temperature as same as methyl carbons. From the result of quaternary carbons, different fractions having slower and faster T_1 would be existed in AG-041R, suggesting the inhomogeneity of the amorphous state.

Fig. 8 shows the relaxation time of individual benzene ring carbons as a function of temperature. The relaxation curve of each carbon was not fitted in two components but one component equation, and the value was constant from 60 to 80 °C and from 100 to 110 °C, respectively. This finding was in accord

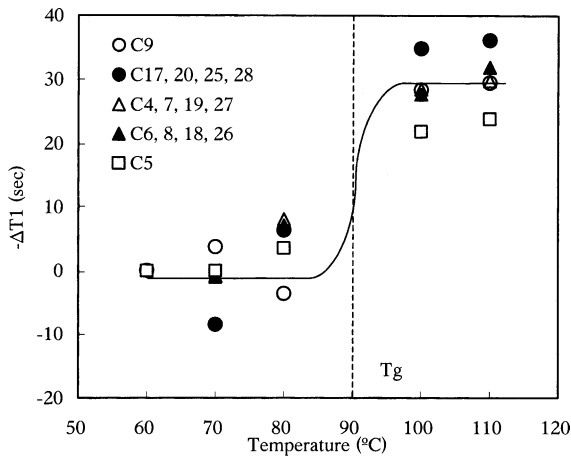


Fig. 8. Change in the relaxation time of each carbon of benzene ring as a function of temperature.

with the T_g data obtained by DSC. The benzene rings are main skeleton structure and may interact with one another by van der Waals force, therefore, it was considered to be predominantly involved in glass transition of AG-041R. Consequently, the measurement of T_1 by solid-state NMR is helpful to evaluate the T_g of amorphous pharmaceuticals precisely.

There are several kinds of carbons that showed two relaxation components, suggesting fast and slow relaxation processes. As shown in Fig. 9 and Table 1, drastic change of T_1 at temperature of T_g was not observed in quaternary carbon C3. Moreover T_1 of C3 consists of two components, resulting the existence of two relaxation processes, fast and slow components. This fact means the heterogeneity in the molecular mobility is existed in AG-041R,

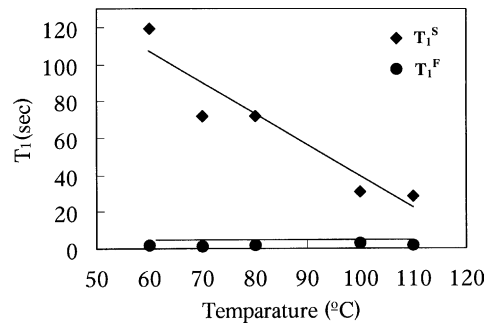


Fig. 9. Relaxation time of slow and fast relaxation processes of quaternary carbon C3 as a function of temperature.

suggesting there would be two components having high and low molecular mobility. Since AG-041R has two large side chains, (4-methylphenyl)ureide and (4-methylphenyl)aminocarbonyl methyl, the molecule might interact in different way. The mobility difference in AG-041R would be caused by the difference in molecular interaction; inter- or intramolecular hydrogen bonding between the side chains. The T_1 of the slower component (T_1^S) gradually decrease depending on temperature. However, the faster component (T_1^F) was not changed throughout the relaxation measurement, and the ratio of two components was independent of the experimental temperature. C3 bonded with (4-methylphenyl)ureide and (4-methylphenyl)aminocarbonyl methyl having the interaction between these two side chains, there would be some way of the interaction, and hence this carbon was considered to be in different molecular states. The constant ratio of heterogeneity suggested that the interaction of inter/intramolecule might not

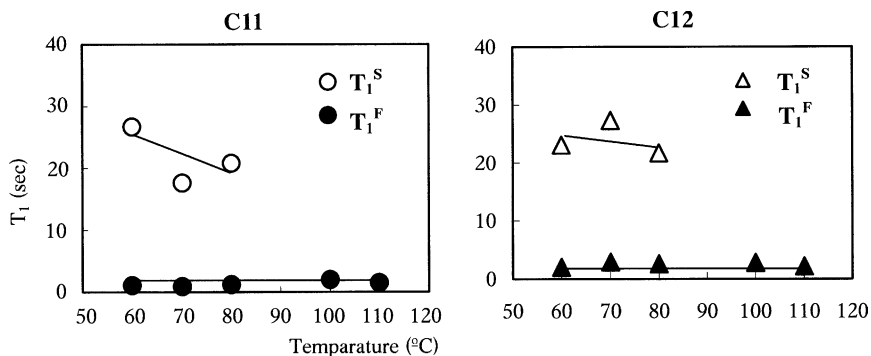


Fig. 10. The relaxation behavior of acetal group (C11, 12) as a function of temperature.

change, and the hydrogen bonding would be strong and effective enough to keep AG-041R amorphous even in the supercooled liquid.

Fig. 10 shows the temperature dependency on the relaxation time of acetal groups, C11 and 12, of AG-041R. These carbons showed two relaxation components below T_g , showing the heterogeneity like the quaternary carbon, but the slower part of relaxation was diminished above T_g and only the faster part of relaxation was observed. The mobility of acetal group might be restricted below T_g , and then significantly increased above T_g due to the medium size of functional group. This suggests that the molecular mobility of acetal group became faster and this functional group was changed to homogeneous state in supercooled liquid state.

Fig. 11 shows the molecular mobility of methyl group, C13, 21, and 29, as a function of temperature. Here, all were determined as a single component. The T_1 of C13 was small and completely independent of the temperature. The T_1 of C21 and 29 was slightly long and dependent on the temperature, however, observed value was not drastically changed at T_g . The C13 of acetal carbon is a terminal of two branches of ethoxy group and might be flexible because each branch does not interact with each other or in the vicinity of another molecules. Therefore, the mobility of

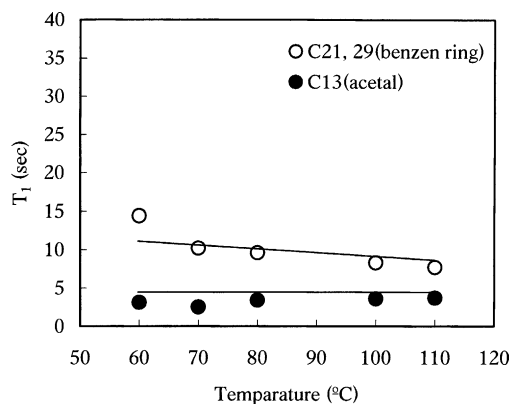


Fig. 11. The relaxation behavior of methyl group (C13, 21, 29) as a function of temperature.

C13 was high even below the T_g and independent of temperature. The methyl carbons C21 and 29 bonded with benzene rings might be slightly restrict their mobility.

Fig. 12 shows the relaxation time change of three carbonyl carbons, C2, 15, and 23, as a function of temperature. The T_1 of each carbonyl carbon was only gradually decreased depending on temperature, moreover, no drastic change of T_1 occurred at T_g . The curve fitting analysis of these carbons, however, was done as not two components but one, so it was considered to

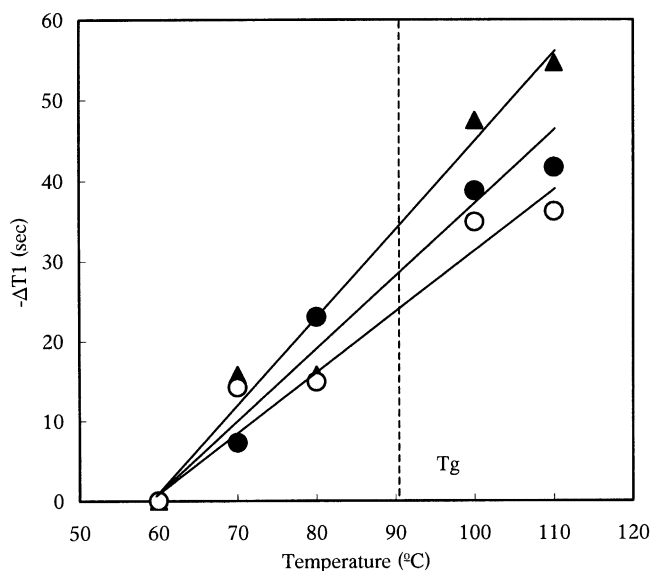


Fig. 12. Change in the relaxation time of three carbonyl carbons (C2, 15, 23) as a function of temperature; (▲) C15, (●) C23, (○) C2.

Table 2
Molecular mobility, number of carbon, and inhomogeneity of each functional group of AG-041R

Functional group	Mobility		Number of carbon	Inhomogeneity
	Below T_g	Above T_g		
Methyl, C13, 21, 29	High	High	4	No
Methylene, C10, 22	High/low	High	2	Yes
Acetal, C11, 12	High/low	High	3	Yes
Benzene ring, C4–9, 17–20, 25–28	Low	High	18	No
Quaternary, C3	High/low	High/low	1	Yes
Carbonyl, C2, 15, 23	Low	Low	3	No

have homogeneity. Since the extent of the change in the relaxation time ($-\Delta T_1$) of each carbons was in the order of $C15 > C23 > C2$, the molecular constraint of the functional group including C2 was stronger than that including C15, and hence the intensity of hydrogen bonding of C2 would be stronger than that of C15. As described in previous section, the intramolecular hydrogen bonding was formed between N14, H, and C23=O, and the intermolecular hydrogen bonding was formed between N16, 24, H, and C2, 15=O. Moreover, the hydrogen bonding with N24 was stronger than that with N14, suggesting the N24 would be bound to C2 and N16 would be bound to C15. As shown in Fig. 12,

there was no significant change of $-\Delta T_1$ was observed at T_g , consequently, the hydrogen bonding might be effective even above T_g . The inter- and intramolecular interaction was considered to retain even in a supercooled liquid state due to hydrogen bonding, therefore, this molecule might be stable in the supercooled liquid.

As described above, the T_g observed by DSC was the temperature that benzene ring carbons start to move, and other carbons have no drastic temperature dependency at T_g . Thus, from the view point of molecular mobility, all of the carbons might not start to move drastically at 90 °C. Table 2 shows

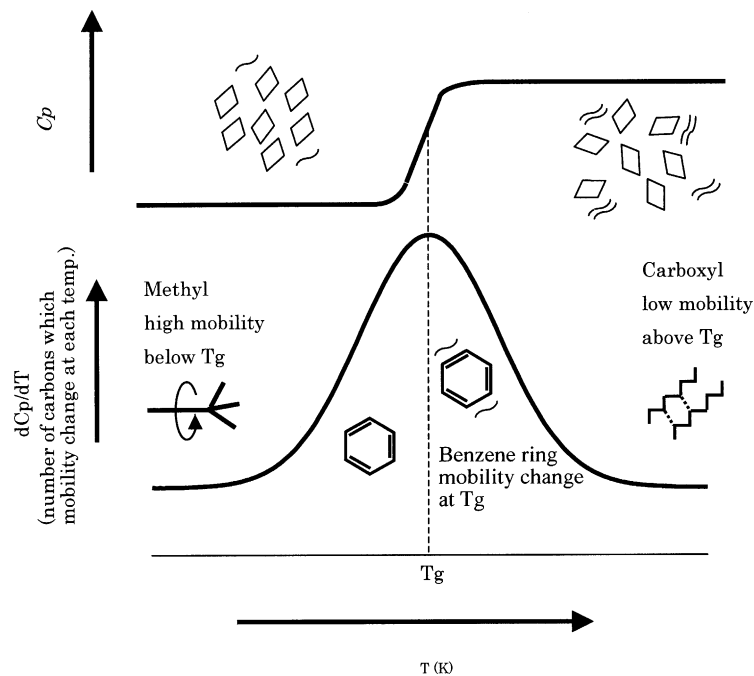


Fig. 13. Schematic representation of the molecular mobility of carbons below and above glass transition temperature.

the molecular mobility, number of carbon, and inhomogeneity of each functional group of AG-041R. There were different groups of carbon in terms of temperature dependency of T_g ; one is a type, such as the methyl carbons. The molecular mobility of methyl carbon was high below T_g and homogeneous, suggesting no contribution to the macroscopic glass transition phenomena observed by DSC. Methylene and acetal carbons showed the inhomogeneity at the temperature below T_g , however, the homogeneity was achieved above T_g affecting some extent to mobility change at T_g for the carbons belong to benzene ring, the molecular mobility was drastically changed at T_g . The number of carbons of this group was almost 60% of whole molecule, suggesting the predominant effect to the macroscopic T_g . On the other hand, the quaternary and carbonyl carbons showed low molecular mobility above T_g . These carbons would not contribute to the macroscopic T_g of AG-041R, but this group would be important for the stabilization of amorphous state resulting from the existence of hydrogen bondings. Fig. 13 shows schematic representation of the molecular mobility of carbons below and above glass transition temperature. The structure that contributes glass transition phenomena would be the main skeleton structure, such as benzene ring. While small group, like methyl, start to move at lower temperature, and restricted groups, such as carbonyl, interacted inter- and/or intramolecularly, suggesting no contribution to the macroscopic T_g of AG-041R. The lower curve illustrates the change in dC_p/dT by temperature. As shown in Table 2, there are six functional groups having the different temperature dependency. The macroscopic glass transition phenomena would be made up of the mobility changes of each functional group at each temperature. Therefore, the value dC_p/dT would be correlated to the number of carbons which mobility change at each temperature.

4. Conclusion

The investigation of the molecular mobility of amorphous pharmaceuticals, so far, has been conducted as measurement of T_g and enthalpy relaxation by means of DSC. The large pharmaceutical molecule, however, does not move all functional groups at narrow tem-

perature range around T_g . In order to understand the true molecular mobility, it is important to investigate the microscopic mobility, because the T_g observed by DSC would prove to be only macroscopic T_g , that is, a summation of the relaxation behavior of whole structure.

The inter- and intramolecular interaction were confirmed by spectroscopic analysis, therefore, the molecular mobility of AG-041R was restricted even at supercooled liquid state. The interaction might be caused between functional groups because of larger molecular size. The larger molecule would be heterogeneous structurally and its T_g may show some temperature distribution depending on the microscopic structure. The T_g is considered from the aspect of molecular mobility; overall structure of the molecule does not increase its mobility drastically at T_g as do some other groups present in the structure. NMR method would be useful and helpful to investigate the physicochemical stability of amorphous pharmaceuticals, which will be developed increasingly in future.

Acknowledgements

The authors thank Mr. Tetsu Matsuura and Mr. Kenji Kamata, Chugai Pharmaceutical Co. Ltd., for their helpful assistance and discussions.

References

- Aso, Y., Yoshioka, S., Kojima, S., 2000. Relationship between the crystallization rates of amorphous nifedipine, phenobarbital, and flopropione, and their molecular mobility as measured by their enthalpy relaxation and ^1H NMR relaxation times. *J. Pharm. Sci.* 89, 408–416.
- Ding, X.Q., Lindstrom, E., Hakanson, R., 1997. Evaluation of three novel cholecystokinin-B/gastrin receptor antagonists: a study of their effects on rat stomach enterochromaffin-like cell activity. *Pharmacol. Toxicol.* 81, 232–237.
- Fukui, Y., Kinoshita, T., Maekawa, A., Okada, S., Waki, S., Hassan, H., Okamoto, H., Chiba, T., 1998. Regeneration gene protein may mediate gastric mucosal proliferation induced by hypergastrinemia in rats. *Gastroenterology* 115, 1483–1493.
- Hancock, B.C., Dupuis, Y., Thibert, R., 1999a. Determination of the viscosity of an amorphous drug using thermomechanical analysis (TMA). *Pharm. Res.* 16, 672–675.
- Hancock, B.C., Shamblin, S.L., Zografu, G., 1999b. Molecular mobility of amorphous pharmaceutical solids below their glass transition temperatures. *Pharm. Res.* 12, 799–805.

- Jaeghere, F.D., Allemann, E., Kubel, F., Galli, B., Cozens, R., Doelker, E., Gruny, R., 2000. Oral bioavailability of a poorly water soluble HIV-1 protease inhibitor incorporated into pH-sensitive particles: effect of the particle size and nutritional state. *J. Control. Release* 68, 291–298.
- Matsumoto, T., Zografi, G., 1999. Physical properties of solid molecular dispersions of indomethacin with poly(vinylpyrrolidone) and poly(vinylpyrrolidone-co-vinyl-acetate) in relation to indomethacin crystallization. *Pharm. Res.* 16, 1728–1772.
- Moynihan, C.T., Easteal, A.J., Wilder, J., Tucker, J., 1974. Dependence of the glass transition temperature on heating and cooling rate. *J. Phys. Chem.* 78, 2673–2677.
- Schmitt, E.A., Law, D., Zhang, G.G., 1999. Nucleation and crystallization kinetics of hydrated amorphous lactose above the glass transition temperature. *J. Pharm. Sci.* 83, 291–296.
- Shamblin, S.L., Hancock, B.C., Duplix, Y., Pikal, M.J., 2000. Interpretation of relaxation time constants for amorphous pharmaceutical systems. *Int. J. Pharm. Sci.* 89, 417–427.
- Wang, W., Ronald, J.P., Grant, D.M., 1996. Glass and crystal formation in binary aromatic mixtures: a mechanism for reducing spin–lattice relaxation times. *J. Phys. Chem.* 100, 18550–18553.
- Williams, G., Watts, D.C., 1970. Non-symmetrical dielectric relaxation behavior arising from a simple empirical decay function. *Trans. Faraday Soc.* 66, 80–85.
- Yamaguchi, T., Nishimura, M., Okamoto, R., Takeuchi, T., Yamamoto, K., 1992. Glass formation of 4''-O-(4-methoxyphenyl) acetylosin and physicochemical stability of the amorphous solid. *Int. J. Pharm.* 85, 87–96.
- Yoshioka, M., Hancock, B.C., Zografi, G., 1994. Crystallization of indomethacin from the amorphous state below and above its glass transition temperature. *J. Pharm. Sci.* 83, 1700–1705.
- Yoshioka, S., Aso, Y., Kojima, S., 1999. The effect of excipients on the molecular mobility of lyophilized formulations, as measured by glass transition temperature and NMR relaxation-based critical mobility temperature. *Pharm. Res.* 16, 135–140.